Journal of Materials Chemistry C, Volume 7, Issue 45, 2019, Article number 14109
DOI:10.1039/c9tc05208a

Tailoring the electrocaloric effect of $Pb_{0.78}Ba_{0.2}La_{0.02}ZrO_3$ relaxor thin film by GaN substrates

Biaolin Peng[1,2,3,4*§], Jintao Jiang[1§], Silin Tang[1], Miaomiao Zhang[1], Laijun Liu[5], Bingsuo Zou[1,3,4], Glenn J.T. Leighton[2], Christopher Shaw[2], Nengneng Luo[1,4], Qi Zhang[2*], Wenhong Sun[1,3,4*]

[1]Center on Nanoenergy Research, School of Physical Science & Technology, Guangxi University, Nanning 530004, China

[2]Department of Manufacturing and Materials, Cranfield University, Cranfield, Bedfordshire, MK43 0AL, United Kingdom

[3]Reserch Center for Optoelectronic Materials and Devices, School of Physical Science & Technology, Guangxi University, Nanning 530004, China

[4]Guangxi Key Laboratory of Processing for Non-ferrous Metal and Featured Materials, Guangxi University, Nanning 530004, China

[5]Guilin University of Technology, School of Materials and Engineering, Guilin, Guangxi, 541004, China

[*]Correspondence to: pengbl8@126.com, q.zhang@cranfield.ac.uk, 20180001@gxu.edu.cn

[§]These authors contributed equally to this work.

Abstract: Electrocaloric (EC) effect in ferroelectric/antiferroelectric thin films has been widely investigated due to the potential applications in solid state cooling devices. It is demonstrated that the EC effect of the $Pb_{0.78}Ba_{0.2}La_{0.02}ZrO_3$ (PBLZ) relaxor thin films prepared by using a sol-gel method strongly depends on the substrates. The maximum ΔT of PBLZ thin films deposited on the Pt(111)/TiO_x/SiO_2/Si(100) (Pt), the $LaNiO_3$/Pt(111)/TiO_x/SiO_2/Si(100) ($LaNiO_3$/Pt), the $LaNiO_3$/n-type GaN ($LaNiO_3$/n-GaN) and the $LaNiO_3$/p-type GaN ($LaNiO_3$/p-GaN) substrates are ~ 13.08 K, 16.46 K, 18.70 K, and 14.64 K, respectively. Moreover, negative EC effects in a broad temperature range (~ 340 K to 440 K) could be obtained in the thin films deposited on $LaNiO_3$/n-GaN and $LaNiO_3$/p-GaN substrates, which is ascribed to the higher proportion of orthorhombic antiferroelectric phase to rhombohedral ferroelectric phase induced by GaN substrates. These results indicate that tailoring the EC effects by the substrates could provide a new strategy in designing the EC cooling device with high cooling efficiency.

Keywords: electrocaloric effect, thin film, PBLZ, substrate

1. Introduction

Recently, the electrocaloric (EC) refrigeration have drawn more and more research attentions due to the breakdown of the large ΔT in ferroelectric/antiferroelectric (FE/AFE)[1-10], and is considered as a competitive solid-state cooling technology for microelectronic systems such as the computers and smart phone[11-16]. It refers to an induced change in the adiabatic temperature (ΔT) or isothermal entropy (ΔS) of a polarizable dielectric material upon the application or withdrawal of an electric field[1,5,17]. The ΔT and the ΔS are very sensitive to many factors such as the applied electric field, thickness, phase structure and orientation, etc[18,19].

With the development of the preparation technology of ceramic thin film with high quality, larger electric breakdown strength can be achieved. Triggered by the giant EC effect (ΔT ~ 12 K) reported by Mischenko[1] et al., a lot of theoretical and experimental studies have been carried out. No matter the bulk ceramics or the thin films, the EC effect all have been improved significantly. For example, a large EC effect with ΔT ~ 2.05 K at 40 kV/cm is obtained in the $Pb_xSr_{1-x}TiO_3$ bulk ceramics near the phase transition temperature[20]. A giant EC effect with ΔT ~ 45.3 K at 598 kV/cm is achieved in the $Pb_{0.8}Ba_{0.2}ZrO_3$ thin films with the coexistence of antiferroelectric and ferroelectric phase[17]. A large EC effect with ΔT ~ 14.5 K at 600 kV/cm is obtained in the $0.67PbMg_{1/3}Nb_{2/3}O_3$-$0.33PbTiO_3$ thin films with a highly (001)-orientation[21].

In addition to the great progress made in the above positive EC effects, the progress in negative EC effect has also been made rapidly. For example, a giant negative EC effect with ΔT ~ - 52.2 K at low temperatures (150 - 210 K) were observed in the $PbZr_{0.53}TiO_{0.47}/CoFe_2O_4$ ferroelectric/ferromagnetic multilayer nanolaminate[22], and very recently a giant EC effect with ΔT ~ - 42.5 K at 436 K were demonstrated for the $0.5(Ba_{0.8}Ca_{0.2})TiO_3$–$0.5Bi(Mg_{0.5}Ti_{0.5})O_3$ lead-free relaxor ferroelectric thin film due to the electric field induced structural phase transition (nanoscale tetragonal and orthorhombic to rhombohedral)[23].

Although most of research work about the EC effects are reported in thin films deposited on the well-known Pt/TiOx/SiO_2/Si substrate, some EC effects have also been reported in thin films deposited on other substrates. For example, a large EC effect with ΔT ~ 2.13 K at 508 K is obtained in the PMN-PT ferroelectric thin films deposited on Ir/$SrTiO_3$/TiN/Si (001) substrates using pulsed

laser deposition (PLD) method[24]. A large EC effect with ΔT ~ 6.4 K at 471 K was obtained in the $PbZr_{0.95}Ti_{0.05}O_3$ film fabricated on the FTO substrate using a sol-gel method[25]. It is well known that the GaN is one of the third-generation semiconductor materials, and it possesses many new unique features which are not available in traditional silicon-based semiconductor materials, such as high thermal conductivity, good chemical stability (nearly corroded by any acid) and strong anti-irradiation ability, etc. However, as far as we concerned, few research works have been paid attention to the influence of GaN substrate on the EC effects of FE/AFE thin films. Therefore, it is interesting to carry out a research work on it.

In this work, the influence of the substrates on the EC effects of the $Pb_{0.78}Ba_{0.2}La_{0.02}ZrO_3$ (PBLZ) relaxor thin films prepared using a sol-gel method on different four substrates (Pt, $LaNiO_3$/Pt, $LaNiO_3$/n-GaN, and $LaNiO_3$/p-GaN) were studied systematically. Large positive EC effects at room temperature were obtained and the maximum ΔT for the four substrates are ~ 13.08 K, 16.46 K, 18.70 K, and 14.64 K, respectively. Moreover, negative EC effect in a broad temperature (~ 340 K to 440 K) are obtained in the thin films deposited on $LaNiO_3$/n-GaN and $LaNiO_3$/p-GaN substrates, which is attributed to a higher proportion of orthorhombic antiferroelectric phase to rhombohedral ferroelectric phase induced by GaN substrates. These findings make the GaN substrates very attractive in tailoring the EC effect of thin film materials.

2. Method

2.1 Fabrication of PBLZ

PBLZ thin films were prepared by using a sol-gel method as shown in **Fig. S1 a)**. $Pb(CH_3COO)_3$ with 20% excess Pb, $Ba(CH_3COO)_2$ and $C_6H_9O_6La{\cdot}xH_2O$ were dissolved in a mixture of glacial acetic acid and deionized water at 120 ºC. Simultaneously, $Zr(OC_3H_7)_4$ was dissolved in a mixture of glacial acetic and $CH_3COCH_2COCH_3$ at room temperature. The Pb/Ba/La and Zr solution were then mixed and stirred for 30 min at 100 ºC. After that, appropriate additives were added into the mixed Pb/Ba/La/Zr solution. The final concentration of the PBLZ precursor solution was 0.2 M. After the precursor solution was aged for 24 h, the PBLZ thin films were deposited on four different substrates rinsed with acetone and ethanol. These substrates include $Pt(111)/TiO_x/SiO_2/Si(100)$ (abbreviated as

Pt), $LaNiO_3$/Pt(111)/TiO_x/SiO_2/Si(100) (abbreviated as $LaNiO_3$/Pt), $LaNiO_3$/n-type GaN (abbreviate as $LaNiO_3$/n-GaN) and $LaNiO_3$/p-type GaN (abbreviate as $LaNiO_3$/p-GaN). The PBLZ thin films were prepared by using the layer-by-layer annealing mode. Each layer of thin films was dried on hotplate at 350 ºC for 5 min when spin-coated at 4000 rpm for 30 s, and then pyrolyzed on hotplate at 550 ºC for 5 min, and finally was annealed in a tube furnace at 700 ºC for 3 min in air. After that, the above process was repeated for 8 times. The final film thickness was about 280-390 nm, depending on the substrates.

2.2 Fabrication of substrates with $LaNiO_3$ bottom electrodes

Substrates with $LaNiO_3$ bottom electrodes were prepared by using a sol-gel method, as shown in **Fig. S1 b).** $Ni(CH_3COO)_2$ and $La(NO_3)_3$ were dissolved in a mixture of glacial acetic acid, water and formamide (CH_3NO) at room temperature. The final concentration of the $LaNiO_3$ precursor solution was 0.3 M. After the precursor solution was aged for 24 h, 6-layer-$LaNiO_3$ thin films were deposited on Pt(111)/TiO_x/SiO_2/Si(100), n-GaN and p-GaN substrates by using the layer-by-layer annealing mode. Each layer of thin films was dried on hotplate at 180 ºC for 3 min when spin-coated at 4000 rpm for 40 s, and then pyrolyzed on hotplate at 450 ºC for 10 min, and finally was annealed in a tube furnace at 700 ºC for 5 min in air.

2.3 Characterization

The crystallinities of PBLZ thin films were monitored by X-ray diffraction (XRD; Rigaku 9 kW Smartlab, Tokyo, Japan). The cross-sectional morphologies of thin films were examined by scanning electron microscopy (SEM; HITACHI SU8220). The micro-structures of thin films were observed by transmission electron microscopy (TEM; JEOL JEM-2100F). For the measurement of the electrical properties, square Au/Cr top electrodes with a side length of 90 μm were deposited by the RF magnetron sputtering method and using a shadow mask. Polarization-electric field (*P*-*E*) hysteresis loops were obtained by means of a ferroelectric tester (Precision Premier II Radiant Technologies Inc.). All samples were measured by using the top-to-bottom electrode configuration. The temperature of sample was controlled by a thermal controller (THMSG600, Linkam) with an accuracy of 0.1 ℃.

3. Results and discussion

3.1 Structure

Fig. 1a) shows the X-ray diffraction (XRD) patterns of PBLZ thin films deposited on four different substrates. All thin films exhibit good crystallinity and pure perovskite structure. For simplicity, the diffraction peaks were indexed by using the pseudo-cubic structure rather than the orthorhombic or rhombohedral one. The thin film deposited on Pt substrate exhibits a weak (111)-preferred orientation (black curve). In addition to the Rhombohedral ferroelectric (R_{FE}) phase, the orthorhombic antiferroelectric (O_{AFE}) phase (see O_{AFE}(240/004), etc.) can also been observed[26]. The thin film deposited on $LaNiO_3$/Pt substrate exhibits a strong (110)-preferred orientation. The thin film deposited on $LaNiO_3$/n-GaN substrate exhibits (100)-preferred orientation. However, the thin film deposited on $LaNiO_3$/p-GaN substrate exhibits a weak (110)-preferred orientation. Particularly, the intensity of the O_{AFE}(210) superlattice peak of the thin film deposited on $LaNiO_3$/p-GaN substrate is much stronger to that of the thin film deposited on $LaNiO_3$/n-GaN substrate, indicating a higher proportion of orthorhombic antiferroelectric phase to rhombohedral ferroelectric phase. By comparison with the XRD pattern of the pure p-GaN (see **Fig.S2**), it can be found that the O_{AFE}(210) superlattice peak maybe be more easy to be induced by the p-GaN since that it is very close to its characteristic peak ($2\theta \sim 31.25$ °). It should be noted that the (111) peak can also be detected on the thin film deposited on the $LaNiO_3$/p-GaN substrate (**Fig. 1a)**), which is stronger than that on the thin film deposited on $LaNiO_3$/n-GaN substrate, and the intensity becomes more and more weak with the increase of the number of the $LaNiO_3$ layers (see **Fig.S2**).

Fig. 1b shows the cross-sectional transmission electron microscopy (TEM) image of the PBLZ thin film deposited on the $LaNiO_3$/Pt substrate. In the inside of some nanocrystals (~ 20 nm), wide lamellar nanodomains with thickness of ~ 3 nm (blue circles) and narrow lamellar nanodomains with thickness of ~ 1 nm (red dash circles) are clearly visible. Based on the fact that the cubic and hexagonal phases do not exist in the PBLZ relaxor ferroelectric thin film, the rhombohedral ferroelectric phase was identified easily since the corresponding FFT spectrum is a regular hexagonal shape (inset in **Fig. 1b)**)[23]. However, the wide lamellar nanodomains are hard to be identified in the PBLZ thin films deposited on $LaNiO_3$/n-GaN substrate, as shown in **Fig. S3**. The narrow lamellar

nanodomains could be attributed to the antiferroelectric domains, as reported by Viehland in PZT thin film[27]. These results indicated that the thin film deposited on $LaNiO_3$/n-GaN substrate possesses a higher proportion of orthorhombic antiferroelectric phase to rhombohedral ferroelectric phase than that of the thin film deposited on $LaNiO_3$/Pt substrate.

Fig.1 c) and **Fig. S4** show the temperature dependences of the Raman scattering spectra of the PBLZ thin films deposited on the p-GaN substrate and the Pt/$LaNiO_3$ substrate, respectively. Peak 1 (~ 140 cm^{-1}) is the $A_1(TO_1)$ mode. Peak 2 (~ 225 cm^{-1}) is the $A_1(TO_2)$ mode[23]. Peak 4 (~ 417 cm^{-1}), Peak 6 (~ 569 cm^{-1}) and Peak 8 (~ 735 cm^{-1}) are ascribed to the contribution of the substrate[28]. Peak 5 (~ 508 cm^{-1}) is the A_1TO_3/E(TO) which is attributed to the Zr-O stretching vibration[23]. Peak 7 (~ 588 cm^{-1}) is the $A_1(LO_2)$ mode[29]. Peak 9 (~ 840 cm^{-1}) is similar to the cases in the La-doped $Ba(Zr_{0.3}Ti_{0.7})O_3$ and the La-doped $Ba(Zr_{0.2}Ti_{0.8})O_3$ ceramics[30, 31].

The full width at half maxima (FWHM) of each characteristic peak of the PBLZ thin film deposited on p-GaN substrate are summarized in **Fig. S5**. The variation of the FWHM of each characteristic peak is almost invariable. For the thin film deposited on the p-GaN substrate, the peak 3 (~ 311 cm^{-1}) activated by the vibrations of asymmetric B-O phonon in orthorhombic antiferroelectric phase can be observed in the whole measuring temperature range[23]. These results indicate that the distorted polar nanoclusters in the thin film deposited on the p-GaN substrate may be in a dynamic and thermally stable state by interacting with each other with increasing temperature, especially for the orthorhombic phase. However, for the thin film deposited on the Pt/$LaNiO_3$ substrate, the peak 3 (~ 311 cm^{-1}) can be hardly detected in the whole measuring temperature range, and all peaks are broadened and become weaker with the increase of temperature. The result mentioned above further confirmed that the orthorhombic antiferroelectric phase may be easier to be induced in the thin films deposited on GaN substrates than that in thin films deposited on Pt/TiO_x/SiO_2/Si substrate.

The cross-sectional SEM image of the thin film deposited on Pt substrate shows a typical well-developed columnar-like texture (**Fig. 2a**). However, the thin film deposited on $LaNiO_3$/Pt substrate shows a layer structure (**Fig. 2c)**) rather than a columnar-like texture. Both the thin films deposited on $LaNiO_3$/n-GaN and $LaNiO_3$/p-GaN substrates all show an underdeveloped

columnar-like texture (**Fig. 2e)** and **Fig. 2g**)), but the interface between the PBLZ layer and the $LaNiO_3$ layer is unclear for the thin films deposited on $LaNiO_3$/n-GaN. In contrast, it is clearly visible for the thin films deposited on $LaNiO_3$/p-GaN substrates with different layer number of $LaNiO_3$, as shown in **Fig. 2g**), **Fig. S6c) and S6e).** Benefitting from the well-developed columnar-like texture, the thin film deposited on the Pt substrate show large grain size on its surface SEM image (**Fig. 2b**)). However, the thin films on $LaNiO_3$/Pt, $LaNiO_3$/n-GaN and $LaNiO_3$/p-GaN substrates show small grain sizes.

3.2 Electrocaloric

To assess the EC effect in the PBLZ thin films, the *P-E* loops were collected at 10 kHz and at a step of 5 K. To obtain a large ΔT, a conservative electric field below the dielectric breakdown strength (see **Fig. S7.**) is applied. The temperature dependences of the polarization ($P(T)$) at selected electric fields were extracted from the upper branches of the *P-E* loops in $E > 0$ and presented in the lower right insets of **Fig. 3a), 3c), 3e) and 3g)**. The color solid lines in these insets represent fittings of a polynomial of the raw experimental data.

Based on the Maxwell relationship $(\partial P/\partial T)_E = (\partial S/\partial E)_T$, the ΔT and the ΔS of dielectric material can be determined by:

$$\Delta T = -\frac{1}{\rho}\int_{E_1}^{E_2}\frac{T}{C}\left(\frac{\partial P}{\partial T}\right)_E dE \tag{1}$$

$$\Delta S = -\frac{1}{\rho}\int_{E_1}^{E_2}\left(\frac{\partial P}{\partial T}\right)_E dE \tag{2}$$

Where T is the operation temperature, P the maximum polarizations at the applied electric field E, ρ the density, C the heat capacity, and E_1 and E_2 the initial and final applied electric fields, respectively. Based on previous research results, the ρ and C are assumed to be 7.7 g cm^{-3} and 330 J K^{-1} kg^{-1} in the temperature range studied, respectively. The adiabatic temperature change ΔT and entropy change ΔS of the PBLZ thin films are plotted in **Fig. 3b), 3d), 3f), 3h)** and their insets. Not only the ΔT and ΔS of the thin films increase with the increase of the applied electric field, but also the temperature dependences of the ΔT and the ΔS change with the change of the substrate. Two positive EC peaks are observed around the room temperature for the thin films deposited on the Pt substrate and the

$LaNiO_3$/p-GaN substrate. By contrast, the positive EC peaks cannot be visible for the thin films deposited on the $LaNiO_3$/Pt substrate and the $LaNiO_3$/n-GaN substrate due to shift to a lower temperature. The maximum values of the ΔT of the thin films deposited on Pt, $LaNiO_3$/Pt, $LaNiO_3$/n-GaN, and $LaNiO_3$/p-GaN substrates are 13.08 K, 16.46 K, 18.70 K, and 14.64 K, respectively. Obviously, the positive EC effect of the thin film deposited on the $LaNiO_3$/n-GaN is the largest one. These results indicate that the EC effect can be tailored by the strategy of selecting various substrates.

In addition to the positive EC effect around the room temperature, negative EC effect can also be observed at a higher temperature. The thin films deposited on the Pt substrate show the largest negative EC effect, and the ΔT is about - 6.18 K at 1355 kV/cm. The thin film deposited on $LaNiO_3$/Pt substrate exhibits the smallest negative EC effect, and the ΔT is only - 1.63 K at 1010 kV/cm. Although the negative EC effects (< 4 K) of the thin films deposited on the $LaNiO_3$/n-GaN and $LaNiO_3$/p-GaN substrates are smaller to that of the thin film deposited on the Pt substrate, they exhibit a broader temperature range, and ~ 340 K to 433 K and ~ 362 K to 440 K, respectively.

It is believed that the phase structure and the orientation of the thin film together play a very key role on the magic EC effect. Previous research work of ours has been pointed out that a negative *EC* effect can be induced under the trigger of phase-transition (nanoscale tetragonal/orthorhombic to rhombohedral) when applied an electric field along the out-of-plane [111] direction of relaxor thin film. Therefore, it can be believed that the large negative EC effect may be related to the higher (111)-preferred orientation in the thin film deposited on the Pt substrate, as shown in the XRD pattern (**Fig. 1a)**) and the cross-sectional SEM image (**Fig. 2a)**). Meanwhile, the broad negative EC could be related to the higher proportion of orthorhombic antiferroelectric phase to rhombohedral ferroelectric phase in the thin films deposited on $LaNiO_3$/n-GaN and $LaNiO_3$/p-GaN substrates since that the orthorhombic antiferroelectric phase could be easier to be induced on GaN substrates than that on Pt/TiO_x/SiO_2/Si substrate, as confirmed by the Raman scattering spectra (**Fig.1 c)** and **Fig. S4**).

Although the negative EC effect in the thin films deposited on $LaNiO_3$/n-GaN and $LaNiO_3$/p-GaN substrates is not ideal, the ΔT *&* the ΔS can be further enhanced by increasing the

degree of the (111)-preferred orientation. Therefore, it is expected that a large negative EC in a broad temperature range could be achieved in the thin films deposited on GaN substrates. As a result, refrigeration devices with high cooling efficiency in one cycle can be realized by utilizing and combining both the large negative and positive EC effects in the further.

Conclusions

The EC effects of the $Pb_{0.78}Ba_{0.2}La_{0.02}ZrO_3$ (PBLZ) relaxer thin films can be tailor by the substrates, and large ΔT ~ 13.08 K, 16.46 K, 18.70 K and 14.64 K were obtained on thin films deposited on Pt, $LaNiO_3$/Pt, $LaNiO_3$/n-GaN and $LaNiO_3$/p-GaN, respectively. Thin films deposited on $LaNiO_3$/n-GaN and $LaNiO_3$/p-GaN exhibit negative EC effects in a broad temperature range, and ~ 340 K to 433 K and ~ 362 K to 440 K, respectively. The negative EC effects can be ascribed to the higher proportion of orthorhombic antiferroelectric phase to rhombohedral ferroelectric phase induced by GaN substrates. Tailoring the EC effects of the thin films by the substrates could provide a new strategy in designing the EC cooling device with high cooling efficiency.

Acknowledgements

This work was supported by the National Natural Science Foundation of China (51402196), the Guangxi Natural Science Foundation (Grants 2016GXNSFCB380006, 2017GXNSFFA198015), and the Innovation Project of Guangxi Graduate Education (YCSW2019049), the Talent of Guangxi province (Grants T3120099202, T3120097921) and the Asean Young Talented Scientist Program and talent model base (Grant AE31200065).

Reference

1 A. S. Mischenko, Q. Zhang, J. F. Scott, R. W. Whatmore and N. D. Mathur, *Science*, 2006, **311**, 1270-1271.

2 R. Ma, Z. Zhang, K. Tong, D. Huber, R. Kornbluh, Y. S. Ju and Q. Pei, *Science*, 2017, **357**, 1130-1134.

3 S. G. Lu and Q. Zhang, *Adv. Mater.*, 2010, **21**, 1983-1987.

4 B. Lu, P. Li, Z. Tang, Y. Yao, X. Gao, W. Kleemann and S. G. Lu, *Sci. Rep.*, 2017, **7**, 45335.

5 N. Bret, C. Baojin, L. Sheng-Guo, W. Yong, E. Furman and Q. M. Zhang, *Science*, 2008, **321**, 821-823.

6 Q. Li, J. Wang, L. Ma, H. Fan and Z. Li, *Mater. Res. Bull.*, 2016, **74**, 57-61.

7 X. Ren, H. Fan, Y. Zhao and Z. Liu, *ACS Appl. Mater. Interfaces*, 2016, **8**, 26190-26197.

8 P. Ren, Y. Sun, X. Wang, H. Fan and G. Zhao, *Ceram. Int.*, 2017, **43**, 5347-5350.

9 C. Long, W. Ren, Y. Li, L. Liu, Y. Xia and H. Fan, *J. Mater. Chem. C*, 2019, **7**, 8825-8835.

10 C. Long, H. Fan, W. Ren and J. Zhao, *J. Eur. Ceram. Soc.*, 2019, **39**, 4103-4112.

11 H. Gu, X. Qian, X. Li, B. Craven, W. Zhu, A. Cheng, S. C. Yao and Q. M. Zhang, *Appl. Phys. Lett.*, 2013, **102**, 122904.

12 Y. Jia and Y. S. Ju, *Appl. Phys. Lett.*, 2012, **100**, 242901.

13 X. Moya, S. Kar-Narayan and N. D. Mathur, *Nat. Mater.*, 2014, **13**, 439-450.

14 U. Plaznik, A. Kitanovski, B. Rožič, B. Malič, H. Uršič, S. Drnovšek, J. Cilenšek, M. Vrabelj, A. Poredoš and Z. Kutnjak, *Appl. Phys. Lett.*, 2015, **106**, 043903.

15 Z. Sun, Q. M. Wang and W. S. Slaughter, *J. Appl. Phys.*, 2018, **124**, 064503.

16 V. Matjaz, *Prog. Mater Sci.*, 2012, **57**, 980-1009.

17 B. Peng, H. Fan and Q. Zhang, *Adv. Funct. Mater.*, 2013, **23**, 2987-2992.

18 B. Peng, Q. Zhang, X. Li, T. Sun, H. Fan, S. Ke, M. Ye, Y. Wang, W. Lu, H. Niu, X. Zeng and H. Huang, *ACS Appl. Mater. Interfaces*, 2015, **7**, 13512-13517.

19 B. Peng, Q. Zhang, S. Ke, T. Li, H. Niu, X. Zeng, H. Fan and H. Huang, *Ceram. Int.*, 2015, **41**, 9344-9349.

20 P.-Z. Ge, X.-D. Jian, X.-W. Lin, X.-G. Tang, Z. Zhu, Q.-X. Liu, Y.-P. Jiang, T.-F. Zhang and

S.-G. Lu, *J. Mater.*, 2019, **5**, 118-126.

21 Z. Feng, D. Shi and S. Dou, *Solid State Commun.*, 2011, **151**, 123-126.

22 G. Vats, A. Kumar, N. Ortega, C. R. Bowen and R. S. Katiyar, *Energy Environ. Sci.*, 2016, **9**, 1335-1345.

23 B. Peng, Q. Zhang, B. Gang, G. J. T. Leighton, C. Shaw, S. J. Milne, B. Zou, W. Sun, H. Huang and Z. Wang, *Energy Environ. Sci.*, 2019, **12**, 1708-1717

24 Y. He, X. M. Li, X. D. Gao, X. Leng and W. Wang, *Funct. Mater. Lett.*, 2011, **04**, 45-48.

25 Y. Zhao, X. Hao and Q. Zhang, *Ceram. Int.*, 2016, **42**, 1679-1687.

26 B. Peng, Q. Zhang, Y. Lyu, L. Liu, X. Lou, C. Shaw, H. Huang and Z. Wang, *Nano Energy*, 2018, **47**, 285-293.

27 D. Viehland, *Physical review. B, Condensed matter*, 1995, **52**, 778-791.

28 A. Hushur, M. H. Manghnani and J. Narayan, *J. Appl. Phys.*, 2009, **106**, 054317.

29 J. J. Zhu, K. Jiang, G. S. Xu, Z. G. Hu, Y. W. Li, Z. Q. Zhu and J. H. Chu, *J. Appl. Phys.*, 2013, **114**, 153508.

30 S. K. Ghosh, M. Ganguly, S. K. Rout and T. P. Sinha, *Eur. Phys. J. Plus*, 2015, **130**, 68.

31 R. Kumar, K. Asokan, S. Patnaik and B. Birajdar, *J. Alloys Compd.*, 2018, **737**, 561-567.

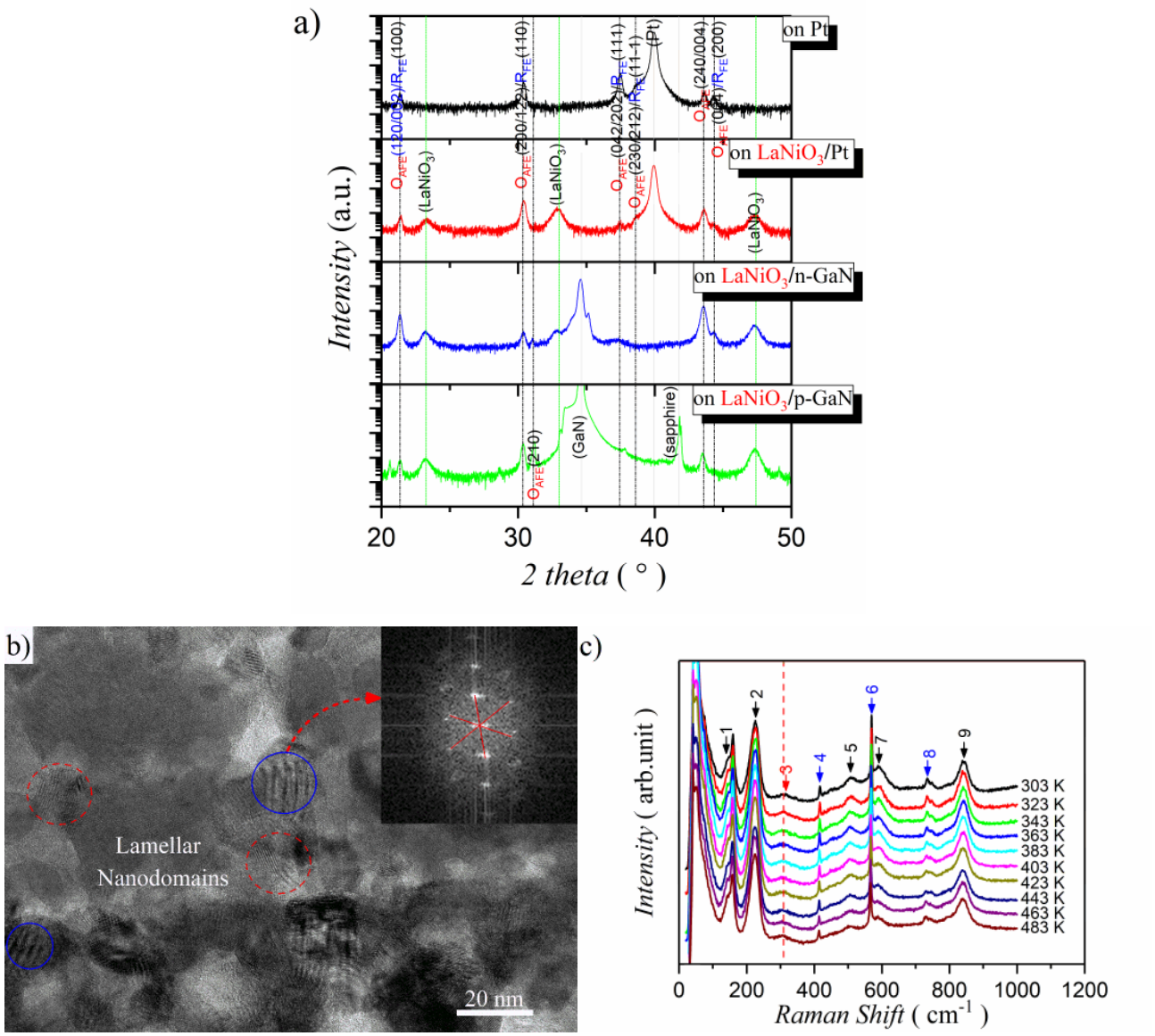

Fig. 1. a) XRD patterns of $Pb_{0.78}Ba_{0.2}La_{0.02}ZrO_3$ (PBLZ) thin films on Pt, $LaNiO_3$/Pt, $LaNiO_3$/p-GaN and $LaNiO_3$/n-GaN substrates. b) Cross-sectional TEM image of thin film on $LaNiO_3$/Pt substrate. Inset: the fast Fourier transform spectrum of the HRTEM image of nanodomains with blue circle as guided by the red arrow. c) Raman scattering spectra of PBLZ thin film on p-GaN substrate. FE: ferroelectric, AFE: antiferroelectric, O: orthorhombic, R: rhombohedral.

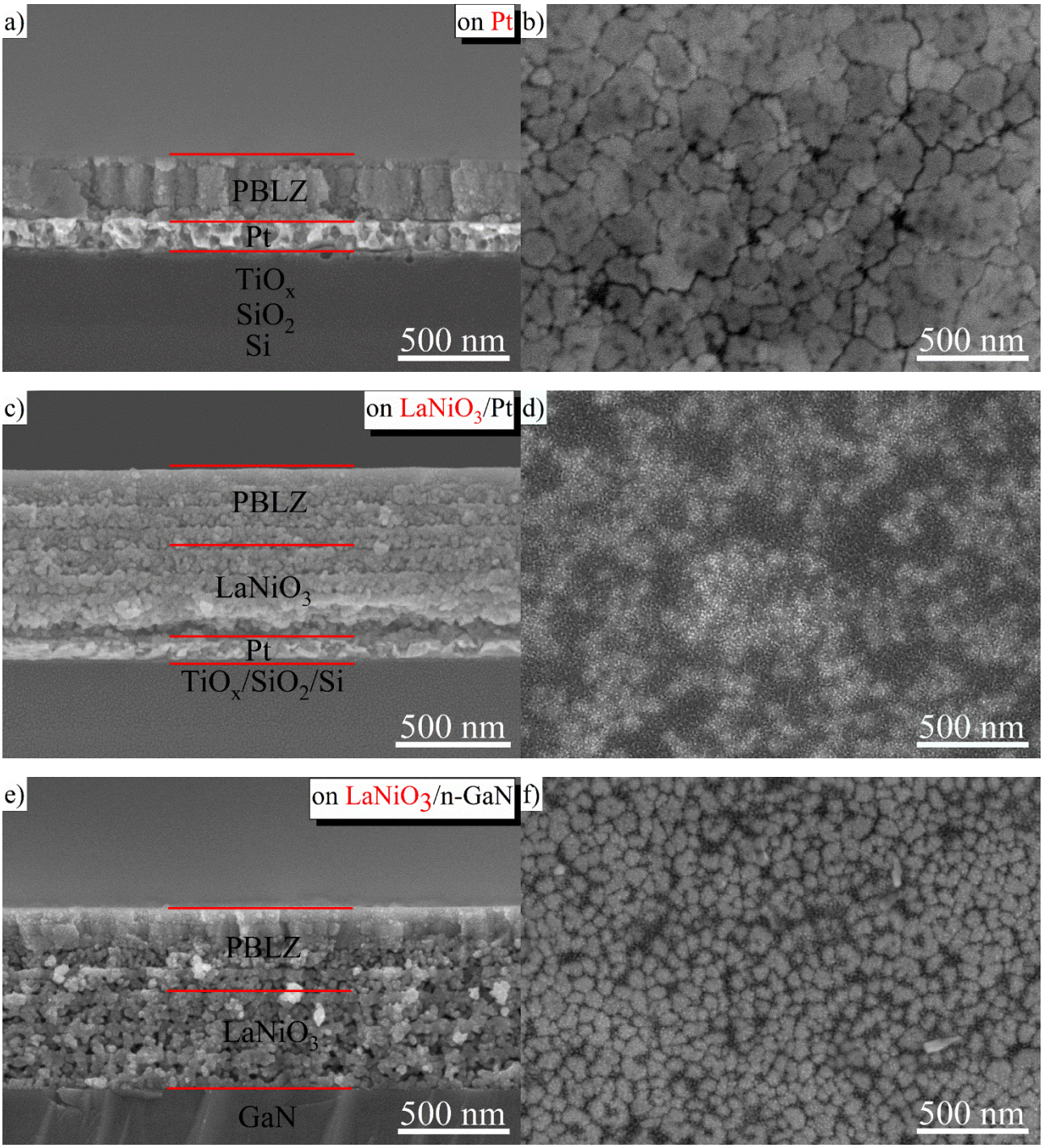
a)
on Pt
PBLZ
Pt
TiOx
SiO2
Si
500 nm
b)
500 nm
c)
on LaNiO3/Pt
PBLZ
LaNiO3
Pt
TiOx/SiO2/Si
500 nm
d)
500 nm
e)
on LaNiO3/n-GaN
PBLZ
LaNiO3
GaN
500 nm
f)
500 nm

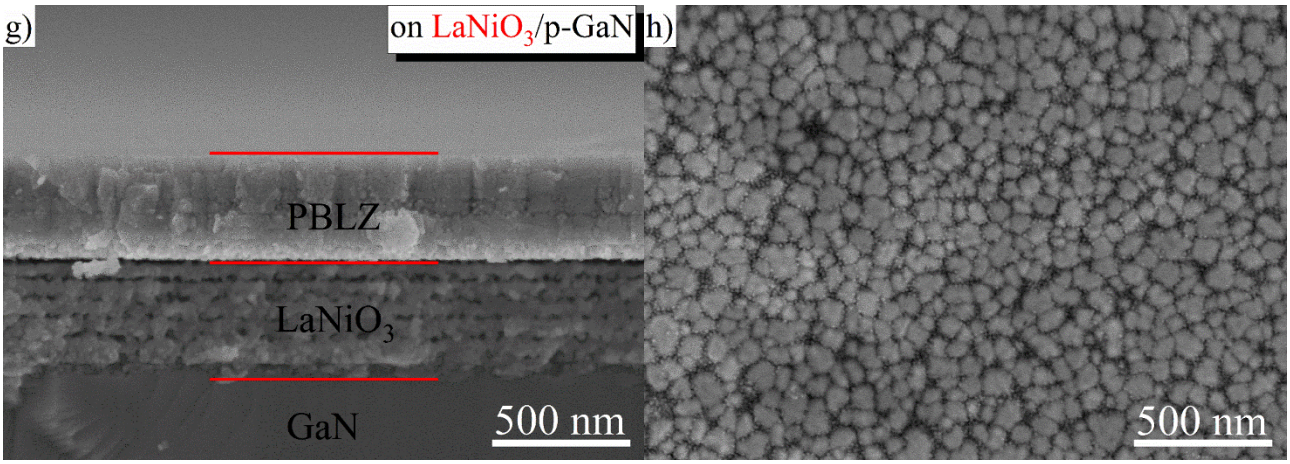

Fig. 2. Cross-sectional and Surface SEM images of PBLZ thin films. (a), (b) on Pt electrode. (c), (d) on $LaNiO_3$/Pt substrate. (e), (f) on $LaNiO_3$/n-GaN substrate. (g), (h) on $LaNiO_3$/p-GaN substrate.

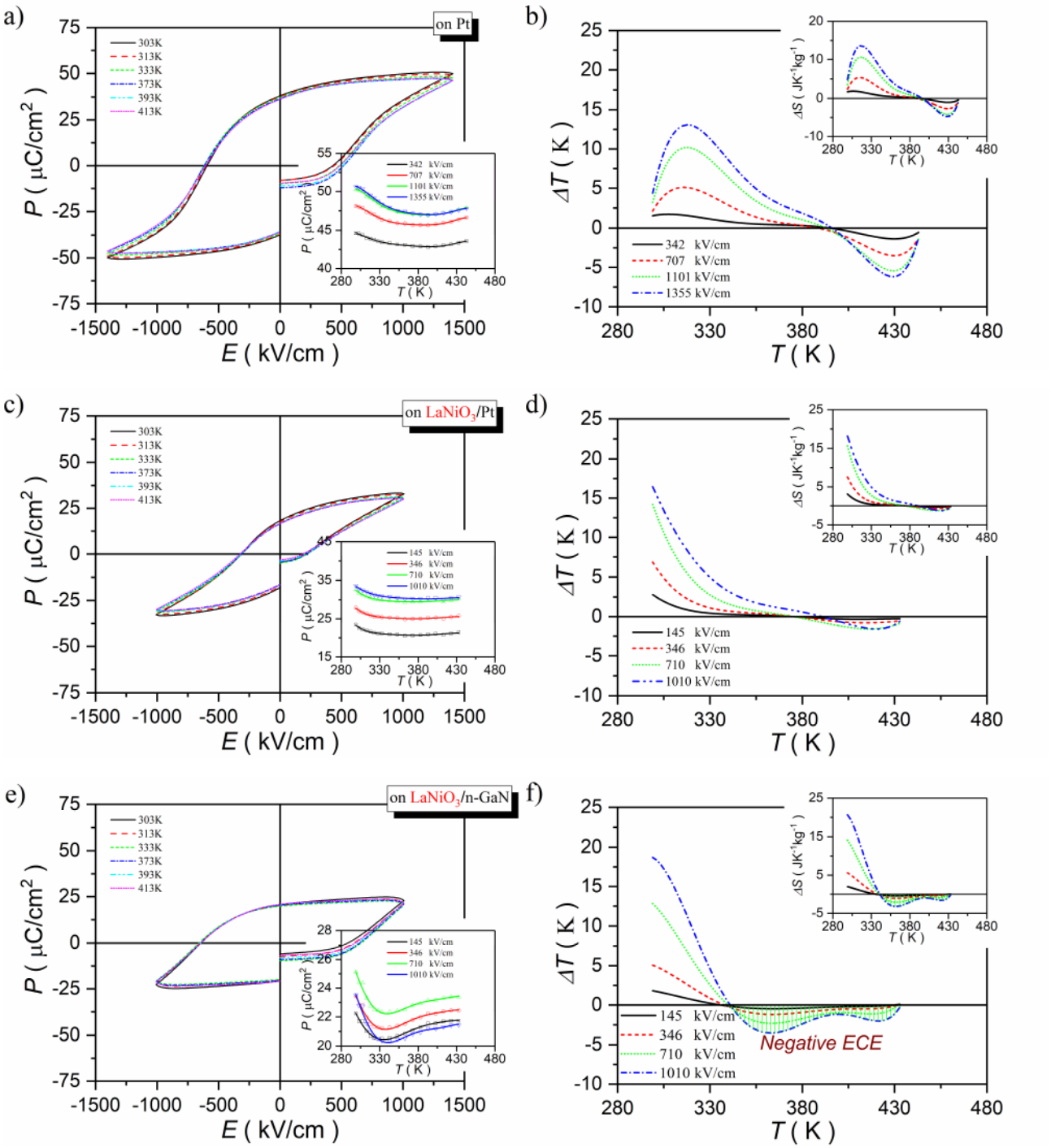
a)
on Pt
303K
313K
333K
373K
393K
413K
P (μC/cm²)
E (kV/cm)
342 kV/cm
707 kV/cm
1101 kV/cm
1355 kV/cm
T (K)
b)
ΔT (K)
ΔS (JK⁻¹kg⁻¹)
c)
on LaNiO3/Pt
145 kV/cm
346 kV/cm
710 kV/cm
1010 kV/cm
d)
e)
on LaNiO3/n-GaN
f)
Negative ECE

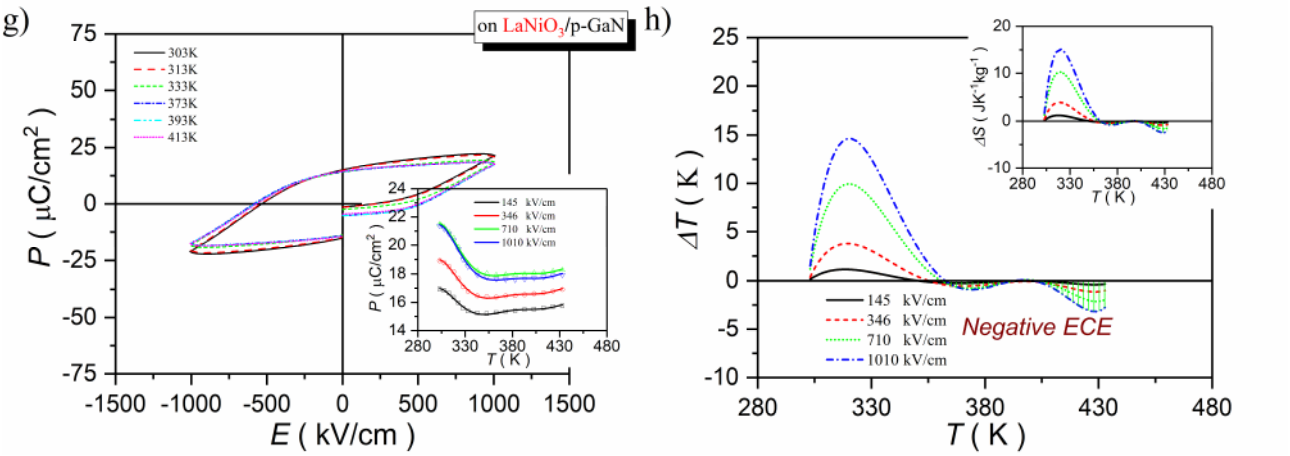

Fig. 3. *P*-*E* loops and the corresponding $\Delta T(T)$ of the PBLZ thin films at selected temperatures at 10 kHz. (a), (b) on Pt substrate. (c), (d) on $LaNiO_3$/Pt substrate. (e), (f) on $LaNiO_3$/n-GaN substrate. (g), (h) on $LaNiO_3$/p-GaN substrate. Insets in (a), (c), (e) and (g): $P(T)$ at selected electric fields. Insets in (b), (d), (f) and (h): $\Delta S(T)$ at selected electric fields.

Supplementary Information for

Tailoring the electrocaloric effect of $Pb_{0.78}Ba_{0.2}La_{0.02}ZrO_3$ relaxor thin film by GaN substrates

Biaolin Peng[1,2,3,4*§], Jintao Jiang[1§], Silin Tang[1], Miaomiao Zhang[1], Laijun Liu[5], Bingsuo Zou[1,3,4], Glenn J.T. Leighton[2], Christopher Shaw[2], Nengneng Luo[1,4], Qi Zhang[2*], Wenhong Sun[1,3,4*]

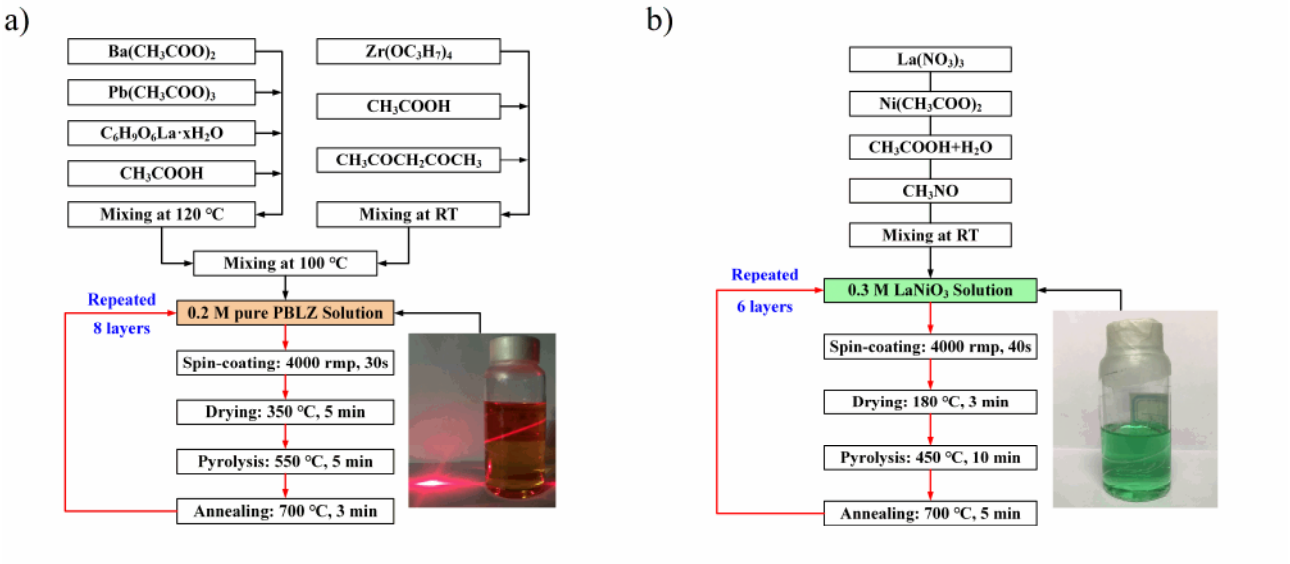

Fig.S1. Flow charts of the preparation of (a) $Pb_{0.78}Ba_{0.2}La_{0.02}ZrO_3$ (PBLZ) thin films and (b) $LaNiO_3$ bottom electrode.

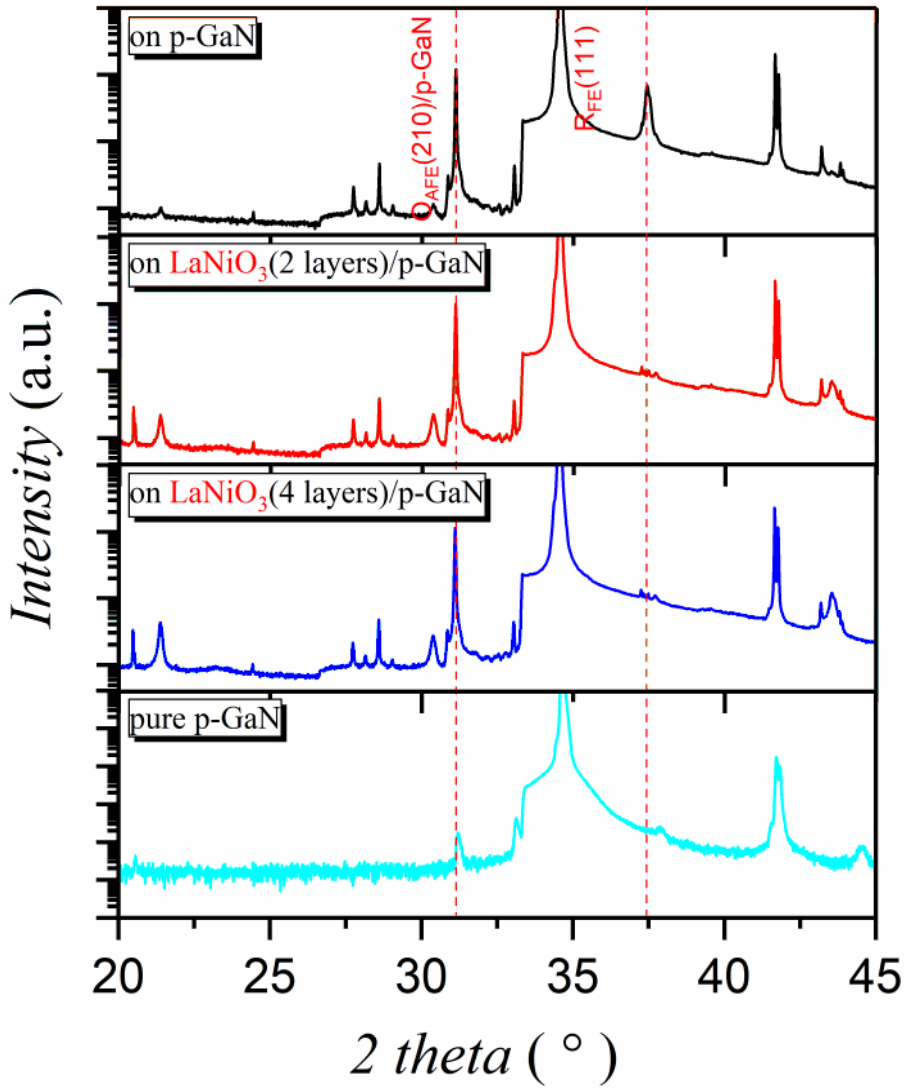

Fig. S2. XRD patterns of the pure p-GaN and PBLZ thin films on p-GaN substrate, $LaNiO_3$ (2 layers)/p-GaN substrate and $LaNiO_3$ (2 layers)/p-GaN substrate.

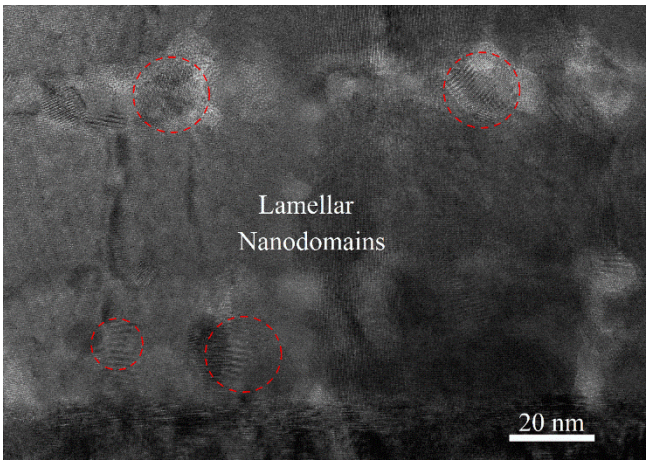

Fig. S3. TEM image of the PBLZ thin film on $LaNiO_3$/n-GaN substrate.

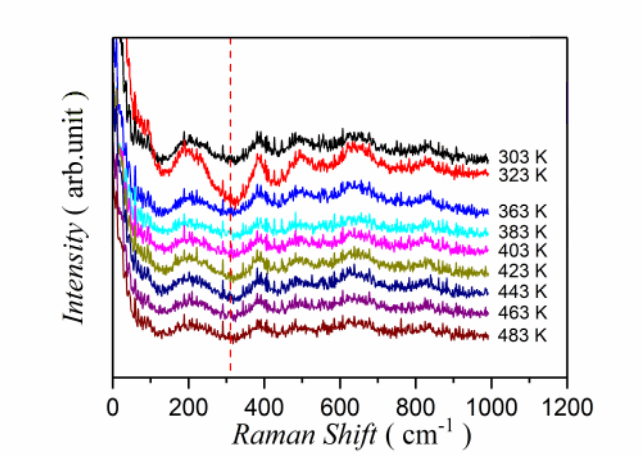

Fig. S4. Raman scattering spectra of the PBLZ thin film on Pt/$LaNiO_3$ substrate at selected temperature.

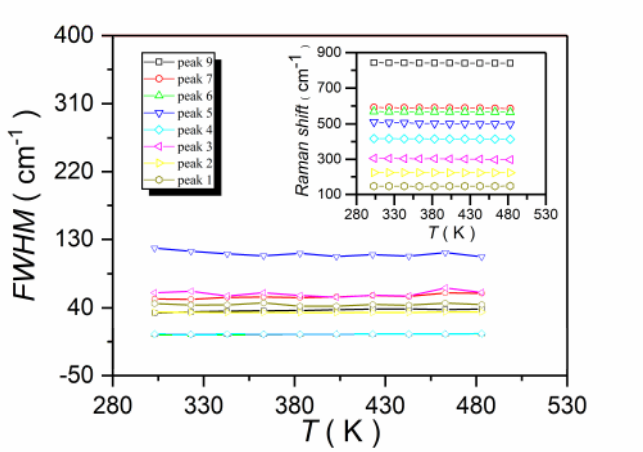

Fig. S5. FWHM of Raman scattering spectra of the PBLZ thin film on p-GaN substrate as a function of temperature of peak 1,2,3,4,5,6,7 and 9. Inset: Raman shift as a function of temperature of peak 1,2,3,4,5,6,7 and 9.

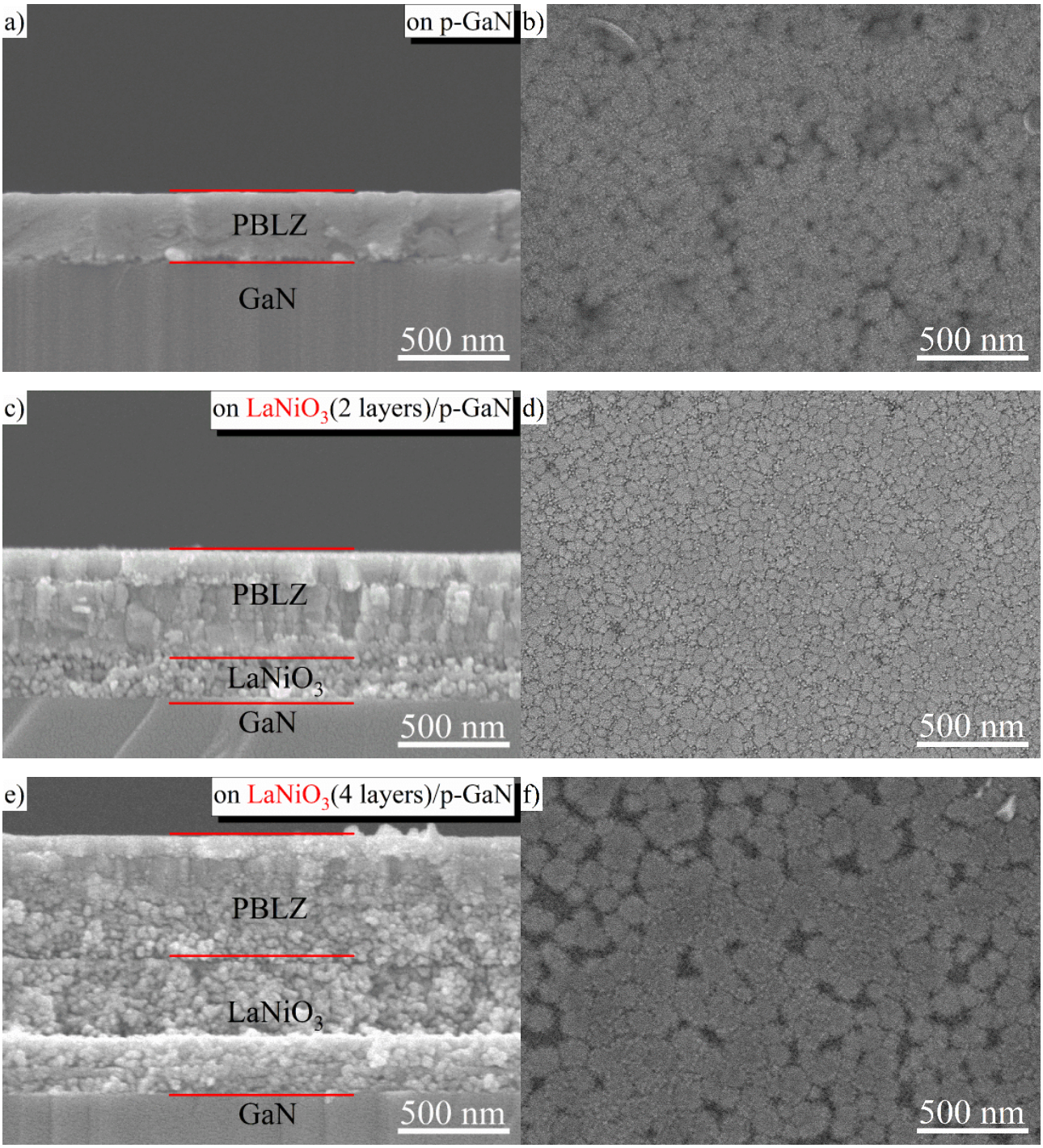

Fig. S6. Cross-sectional and the corresponding surface SEM images of the PBLZ thin films. a), b) on pure p-GaN. c), d) on $LaNiO_3$(2 layers)/p-GaN substrate. e), f) on $LaNiO_3$(4 layers)/p-GaN substrate.

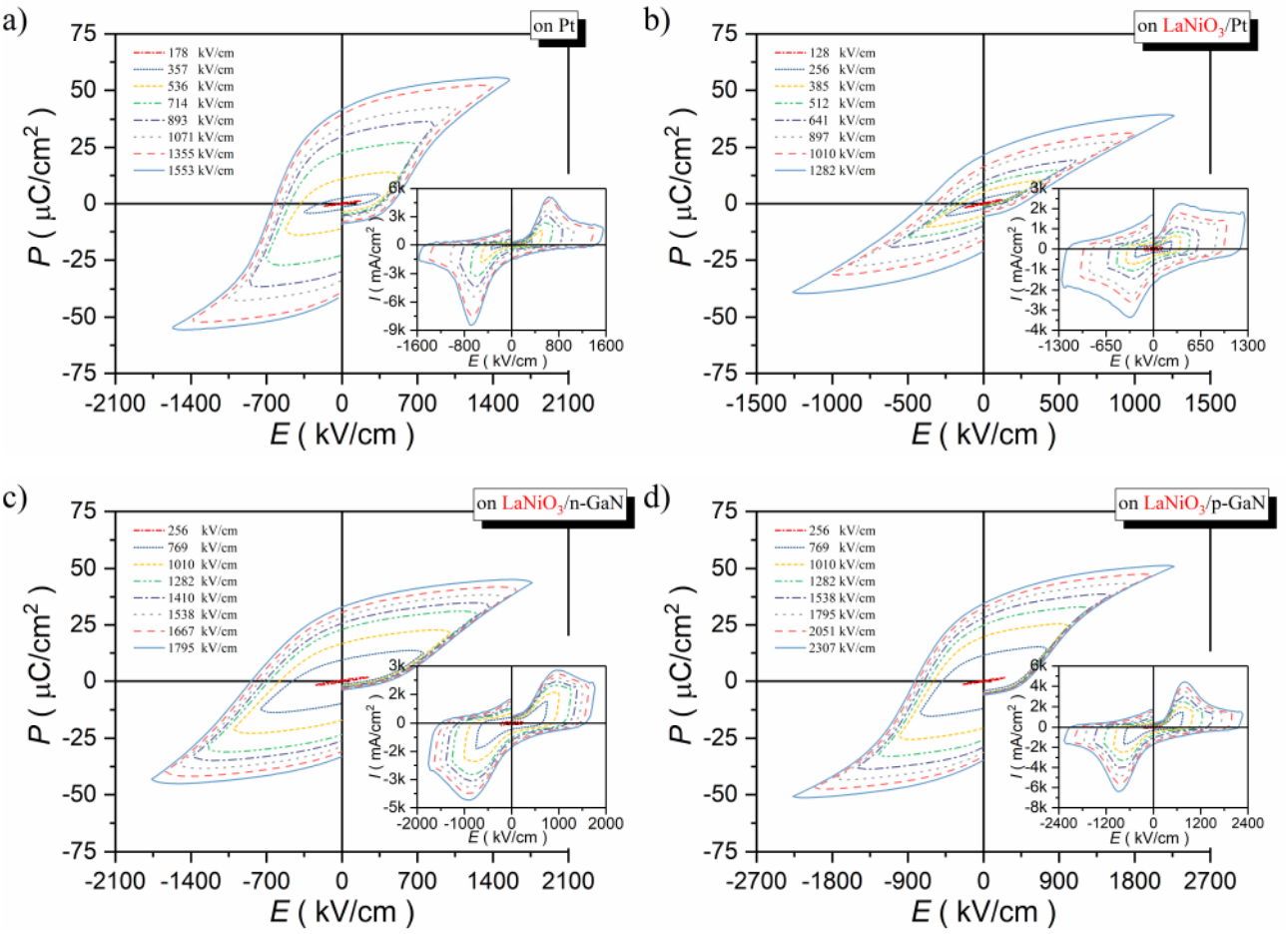

Fig. S7. *P-E* loops of the PBLZ thin films at selected electric fields at 10 kHz (a) on Pt substrate. (b) on $LaNiO_3$/Pt substrate. (c) on $LaNiO_3$/n-GaN substrate. (d) on $LaNiO_3$/p-GaN substrate. Insets in (a), (b), (c) and (d): *I-E* curves at selected electric fields.